

See discussions, stats, and author profiles for this publication at: <https://www.researchgate.net/publication/6333962>

# Solvent Control of Charge Localization in 11-Bond Bridged Dinitroaromatic Radical Anions

ARTICLE *in* JOURNAL OF THE AMERICAN CHEMICAL SOCIETY · JULY 2007

Impact Factor: 12.11 · DOI: 10.1021/ja067088m · Source: PubMed

---

CITATIONS

39

---

READS

25

3 AUTHORS, INCLUDING:



**Stephen F Nelsen**

University of Wisconsin–Madison

**118** PUBLICATIONS **2,237** CITATIONS

SEE PROFILE



**João Paulo Telo**

Technical University of Lisbon

**56** PUBLICATIONS **1,014** CITATIONS

SEE PROFILE

## Solvent Control of Charge Localization in 11-Bond Bridged Dinitroaromatic Radical Anions

Stephen F. Nelsen,<sup>\*,†</sup> Michael N. Weaver,<sup>†</sup> and João P. Telo<sup>\*,‡</sup>

Contribution from the Department of Chemistry, University of Wisconsin, 1101 University Avenue, Madison Wisconsin 53706-1396, and Instituto Superior Técnico, Química Orgânica, Av. Rovisco Pais, 1049-001 Lisboa, Portugal

Received October 3, 2006; E-mail: nelsen@chem.wisc.edu

**Abstract:** The optical spectra of 4,4'-dinitrostilbene (**1**<sup>−</sup>) and 4,4'-dinitrotolane (**2**<sup>−</sup>) radical anions show the narrow band widths and partially resolved vibrational structure exhibited by charge-delocalized dinitroaromatic radical anions in the solvents THF, HMPA, and DMPU (dimethylpropyleneurea). Both show the broad, nearly Gaussian-shaped bands found for charge-localized intervalence compounds in DMF, DMSO, and MeCN, with the transition energy of the band maximum, which equals the vertical reorganization energy ( $\lambda$ ) for localized intervalence compounds, increasing in that order. In contrast, 4,4'-dinitrozobenzene (**3**<sup>−</sup>) remains delocalized in these solvents, although the line width required to simulate the vibrational structure increases by 200 cm<sup>−1</sup> in DMF and 400 cm<sup>−1</sup> in MeCN compared to HMPA. The change from localized to delocalized spectra as a function of solvent establishes the transition energy for which delocalization occurs and demonstrates that, as predicted, the Hush method substantially underestimates the electronic coupling for compounds that lie near the borderline.

## Introduction

Dinitroaromatic radical anions have been of particular interest to ESR spectroscopists since 1960, when Ward<sup>1</sup> published spectra of 1,3-dinitrobenzene radical anion in an ether solvent, under conditions where spin was clearly localized on one nitro group, and Maki and Geske<sup>2</sup> published spectra in acetonitrile, where the spin appeared to be delocalized over both nitro groups. A flurry of activity by several groups for a decade led to general agreement that the solvent was causing the charge to localize on one nitro group, and the suggestion was made that electron transfer between the nitro groups occurred by what is now called an electron-hopping mechanism, for which a symmetrical bridge-centered radical anion is an intermediate.<sup>3</sup> More recently it has been shown that quantum mechanical calculations in fact obtain charge localization for 1,3-dinitrobenzene radical anion in the gas phase and that the optical spectrum of 2,7-dinitronaphthalene radical anion predicts the rate of electron transfer between the nitro groups using the classical Marcus–Hush two-state model<sup>4,5</sup> as accurately as the electron-transfer distance can be estimated, which demonstrates that a sym-

metrical intermediate is not present on the ground-state surface.<sup>6</sup> In the classical two-state model, the shape of the ground-state energy surface can be described using only two energy parameters, the vertical reorganization energy  $\lambda$ , and the off-diagonal electronic coupling matrix element  $H_{ab}$ . When two nitro substituents are placed on aromatic rings in the Kekule substitution pattern that leads to large  $H_{ab}$  values, many dinitroaromatic radical anions are charge-delocalized, with symmetrical instantaneous charge distributions. In terminology developed to describe transition metal-centered examples, charge-delocalized dinitroaromatic radical anions are Robin–Day class III intervalence compounds,<sup>7</sup> that may be usefully described as having two charge-bearing units ( $\mathbf{M} = \text{NO}_2$  in this case) connected by a bridge ( $\mathbf{B}$ ). They are symbolized as having a  $^{-1/2}\mathbf{M}-\mathbf{B}-\mathbf{M}^{-1/2}$  charge distribution (ignoring the fact that a significant amount of the charge will actually be delocalized onto the aromatic bridge), while the charge-localized compounds are class II, having  $^0\mathbf{M}-\mathbf{B}-\mathbf{M}^- \rightleftharpoons ^-\mathbf{M}-\mathbf{B}-\mathbf{M}^0$  charge distributions (also ignoring the smaller amount of charge that is delocalized onto the bridge). For class III compounds, the two  $\mathbf{M}$ -centered charge forms are resonance structures instead of being energy minima for the system. Many class III dinitroaromatic radical anions show quite narrow near-IR absorption bands that exhibit vibrational fine structure.<sup>8</sup> As demonstrated most clearly by the time-dependent Hamiltonian approach introduced

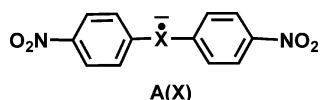
<sup>†</sup> University of Wisconsin.<sup>‡</sup> Instituto Superior Técnico.

- (1) (a) Ward, R. L. *J. Chem. Phys.* **1960**, *32*, 410. (b) Ward, R. L. *J. Am. Chem. Soc.* **1960**, *83*, 1296. (c) Ward, R. L. *J. Chem. Phys.* **1962**, *37*, 1405.  
(2) (a) Maki, A. H.; Geske, D. H. *J. Chem. Phys.* **1960**, *33*, 825. (b) Maki, A. H.; Geske, D. H. *J. Am. Chem. Soc.* **1961**, *83*, 1852.  
(3) Gutch, J. W.; Waters, W. A.; Symons, M. C. R. *J. Chem. Soc. B* **1970**, 1261.  
(4) (a) Marcus, R. A. *J. Chem. Phys.* **1956**, *24*, 966–978. (b) Marcus, R. A.; Sutin, N. *Biochim. Biophys. Acta* **1985**, *811*, 265–322.  
(5) (a) Hush, N. S. *Prog. Inorg. Chem.* **1967**, *8*, 391–444. (b) Hush, N. S. *Coord. Chem. Rev.* **1985**, *64*, 135–157.

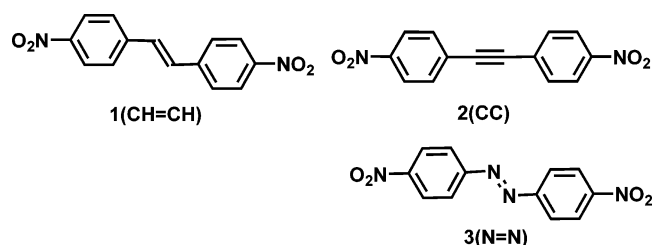
(6) Nelsen, S. F.; Weaver, M. N.; Konradsson, A. E.; Telo, J. P.; Clark, T. *J. Am. Chem. Soc.* **2004**, *126*, 15431–15438.(7) Robin, M. B.; Day, P. *Adv. Inorg. Radiochem.* **1967**, *10*, 247–422.(8) Nelsen, S. F.; Konradsson, A. E.; Weaver, M. N.; Telo, J. P. *J. Am. Chem. Soc.* **2003**, *125*, 12493–12501.

by Heller,<sup>9</sup> observing vibrational fine structure in an absorption band requires that there is a minimum in the excited-state surface near enough the vertical excitation from the ground state that a wave packet promoted to the excited state will recur to its original position within femtoseconds. Vibrational fine structure will not occur for a class II compound, because when  $\lambda > 2H_{ab}$  the ground-state and excited-state minima lie at different points on the horizontal axis (at 0 and 1 on the electron-transfer coordinate for the diabatic surfaces), causing the ground-state energy minimum to lie directly beneath a steeply sloping excited-state energy surface. This produces a very broad, nearly Gaussian-shaped band, which Hush pointed out using a classical analysis and parabolic diabatic states would have a width at half-height of  $(16RT \ln(2) hv_{IV})^{1/2}$ , where  $hv_{IV}$  is the intervalence band maximum transition energy and equals  $\lambda$  in the two-state model.<sup>5</sup> The adiabatic surface minima move toward each other as  $H_{ab}/\lambda$  increases, and a single minimum at 0.5 occurs when  $H_{ab}$  exceeds  $\lambda/2$ , and the system becomes class III. Vibrational fine structure can occur for class III systems because the ground-state and excited-state minima both occur at 0.5 on the horizontal axis of the two-state Marcus–Hush energy diagram.<sup>10</sup> However, as will be emphasized below, the two-state model does not apply unaltered to delocalized systems, including dinitroaromatic radical anions, because the transition being observed is not between the ground and excited states of a single two-state model.<sup>11,12</sup>

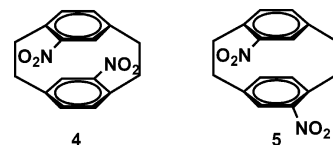
In this work we report the optical spectra and discuss the charge distributions and electronic couplings that they reveal for three Kekule-substituted dinitroaromatic radical anions that have the general structure **A**, where **X** is a two heavy atom bridging unit. These compounds are the radical



anions from **1–3**, which have 11 bonds between their nitrogens, and are Kekule-substituted



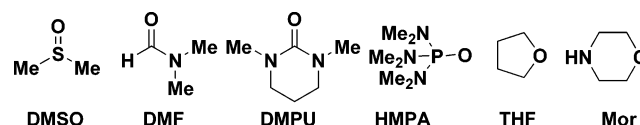
dinitrostilbene, tolane, and azobenzene, respectively. In previous work we found that pseudo-*para*-dinitro[2.2]*para*-cyclophane radical anion (**4**<sup>−</sup>) exhibits the spectrum of a class III compound in hexamethylphosphoramide, HMPA, but that of a localized compound in acetonitrile, and examined its spectrum in several other solvents.<sup>13</sup> In contrast, the pseudo-*ortho* isomer, **5**<sup>−</sup>, shows



the localized spectrum in all solvents examined. We attributed this behavior to **4**<sup>−</sup> lying so close to the class II/class III borderline that changes in the solvent reorganization energy,  $\lambda_s$ , tip it from being localized in the high  $\lambda_s$  solvent MeCN to being delocalized in the low  $\lambda_s$  solvent, HMPA. Considerably smaller electronic coupling is expected for **5**<sup>−</sup> than for **4**<sup>−</sup> because of the different pattern of  $\pi$  system coefficient signs for the two systems, so it does not lie so close to the class II/class III borderline.<sup>13</sup> The larger coupling for **4**<sup>−</sup> arises from through-space interaction of the  $\pi$  systems of paracyclophanes, which precludes quantitative use of the simple Marcus–Hush two-state model, that assumes no overlap between the charge-bearing units. This precludes using Hush's equation to evaluate  $H_{ab}$  from the class II absorption spectra, which was derived for compounds having no overlap between the charge-bearing units. We now report similar behavior for **1**<sup>−</sup> and **2**<sup>−</sup>, which have more conventional  $\pi$  systems having no through-space overlap between the **M** groups.

## Results

**Optical Absorption Spectra.** The optical spectra of **1**<sup>−</sup> and **2**<sup>−</sup> are exceptionally sensitive to solvent, while that of **3**<sup>−</sup> is not, as shown in the plots between 5000 and 15 000 cm<sup>−1</sup> (2000 and 667 nm) for **1**<sup>−</sup> to **3**<sup>−</sup> shown in Figures 1–3.<sup>14</sup> The vibrational fine structure that is observed and the small shift in band maximum with solvent demonstrate that **3**<sup>−</sup> (N=N) remains delocalized even in MeCN. In contrast, **1**<sup>−</sup> (CH=CH) and **2**<sup>−</sup> (C≡C) are charge-localized in MeCN but become delocalized in HMPA and THF, which presumably cause smaller  $\lambda_s$  values. The acronyms used here for solvents are shown below:



## Discussion

**Class III Spectra.** The absorption spectra for the delocalized species in THF are directly compared in Figure 4. From Figures 2 and 4, it seems likely that although the absorption of the delocalized species predominates in the THF spectrum of the C≡C-bridged **2**<sup>−</sup>, it has still not entirely replaced the localized one (which predominates in the top five solvents listed in Figure 2). There might be ion pairing for the delocalized, localized, or both species in nonpolar solvents. These spectra were prepared by sodium amalgam reduction in the presence of cryptand[2.2.2] (**6**), which minimizes ion pairing effects by converting the positive counterion to the rather large encapsulated sodium ion and increases rate constants for intramolecular electron transfer in class II dinitroaromatic radical anions by about an order of magnitude compared to having tetrabutylammonium cation as

- (9) Heller, E. J. *Acc. Chem. Res.* **1981**, *14*, 368–375.  
 (10) (a) Brunschwig, B. S.; Creutz, C.; Sutin, N. *Chem. Soc. Rev.* **2002**, *31*, 168–184. (b) Demadis, K. D.; Hartshorn, C. M.; Meyer, T. J. *Chem. Rev.* **2001**, *101*, 2655–2685. (c) Nelsen, S. F. *Chem. Eur. J.* **2000**, *6*, 581–588.  
 (11) Nelsen, S. F.; Weaver, M. N.; Zink, J. I.; Telo, J. P. *J. Am. Chem. Soc.* **2005**, *127*, 10611–10622.  
 (12) Nelsen, S. F.; Weaver, M. N.; Luo, Y.; Lockard, J. V.; Zink, J. I. *Chem. Phys.* **2006**, *324*, 195–201.  
 (13) Nelsen, S. F.; Konradsson, A. E.; Telo, J. P. *J. Am. Chem. Soc.* **2005**, *127*, 920–925.

- (14) The spectra in Figures 1–3 are “binomial smoothed, 200×” in drawing program IGOR. They have the same general shape as the unsmoothed spectra, but are less noisy, and were used to locate the band maxima reported.

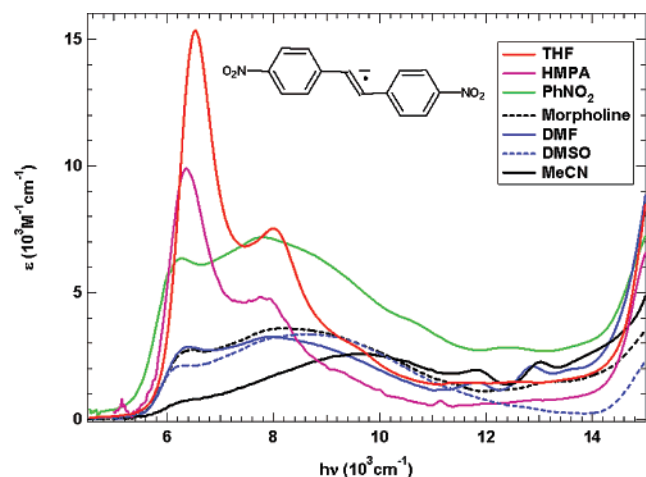


**Figure 1.** Comparison of dinitrostilbene radical anion spectra ( $1^-$ ) in seven solvents.

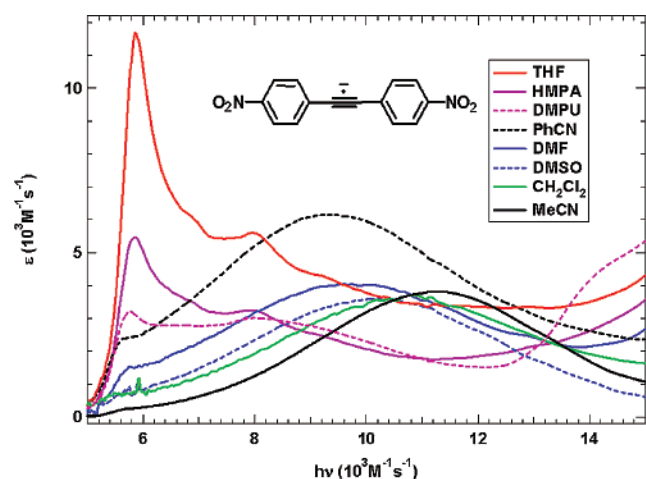
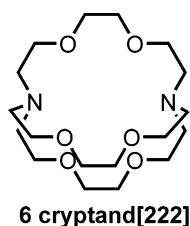


**Figure 2.** Comparison of dinitrotolane radical anion spectra ( $2^-$ ) in eight solvents.



the counterion.<sup>15</sup> Because a charge-localized species would be favored by ion pairing, perhaps small amounts of ion-paired charge-localized material are present, even in the rather polar HMPA, although most of the material is present as delocalized solvent-solvated radical anion.

The properties of the intervalence band for the class III spectra are summarized in Table 1. If the two-state model is applied to the class III spectra,  $H_{ab}(\text{two-state}) = \frac{1}{2}h\nu_{IV}$ . We add  $1^-$ ,  $2^-$ , and  $3^-$  to a plot of  $\ln(\frac{1}{2}h\nu_{IV})$  from the more planar of the previously studied delocalized dinitroaromatic radical anions<sup>11</sup> in Figure 5. Compounds may be selected that make  $\ln(H_{ab}(\text{two-state}))$  nearly linear with the number of bonds between the nitro groups (and hence the distance between the charge-bearing units). These bridges include the 1,4-phenylene, and combinations of 1,4-phenylene, double, and triple bonds, and the Kekule

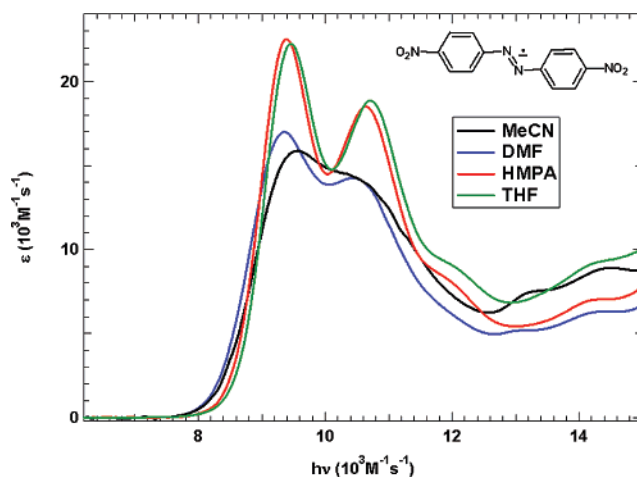


**Figure 3.** Comparison of dinitroazobenzene radical anion spectra ( $3^-$ ) in three solvents.

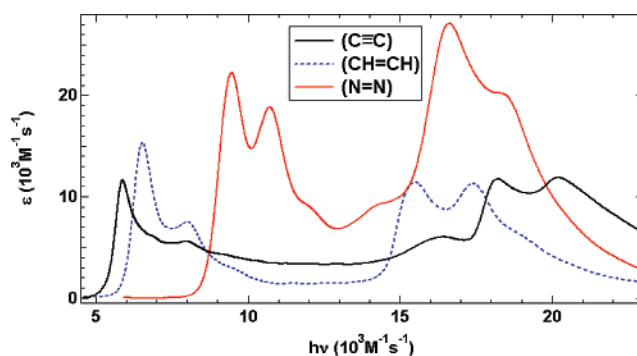


**Figure 4.** Comparison of the first two absorption bands for  $1^-$  to  $3^-$  in THF, where all are delocalized.

pattern 2,6-substituted naphthalene and anthracene rings. These are bridges that have typically been chosen for studies of the distance effect on electronic coupling and have allowed us to continue to believe that the two-state model gives reasonable  $H_{ab}$  values for class III compounds. However, the huge deviations for others of the compounds shown, especially the 1,5-naphthalene, 2,7-biphenylene, and azobenzene-bridged ones, make it clear that the distance between the nitro groups is not the only factor that is determining  $h\nu_{IV}$  for these class III intervalence compounds, which is consistent with  $h\nu_{IV}$  not being simply related to the electronic coupling in these systems.<sup>11</sup>

The (N=N) bridged system  $3^-$  remains delocalized in all solvents studied, so it does not lie as near the class II/III borderline as the hydrocarbon-bridged systems. Its  $h\nu_{IV}$  value is 1.48 times that for  $1^-$ . Introduction of the nitrogens in the bridge lowers the reduction potential for the bridge relative to that of the hydrocarbon bridges of  $1^-$  and  $2^-$ . The importance of lowering the energy gap to the bridge radical ion for increasing electronic coupling of radical anionic intervalence compounds has been discussed in detail by Newton.<sup>16</sup>

Class II spectra are not observed in the solvents studied for  $3^-$ , but increased spectral broadening is obvious in DMF and MeCN compared to HMPA (see Figure 3). The HMPA spectrum could be fit reasonably well by the Abs/emiss/Raman program developed by Zink that is based on a time-dependent Hamil-

(15) Hosoi, H.; Mori, Y.; Masuda, Y. *Chem. Lett.* **1998**, 177.

(16) Newton, M. D. *Chem. Rev.* **1991**, 91, 767–792.



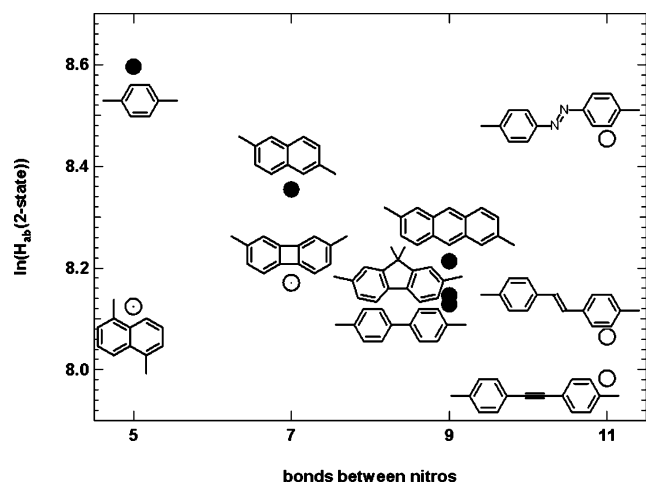


**Figure 5.** Plot of  $\ln(1/2 h\nu_{IV}) = \ln(H_{ab}(\text{two-state}))$  for delocalized dinitroaromatic radical anions.

**Table 1.** First Band Maximum [and Second Vibrational Maximum] Positions ( $\text{cm}^{-1}$ ) for the Class III Spectra of  $1^-$  to  $3^-$ <sup>a</sup>

compd X	THF $h\nu_{IV}, \text{cm}^{-1} (\epsilon_{\text{max}})$	HMPA $h\nu_{IV}, \text{cm}^{-1} (\epsilon_{\text{max}})$	DMPU $h\nu_{IV}, \text{cm}^{-1} (\epsilon_{\text{max}})$
$1^-$ CH=CH	6530 (15 300) [8000 (7520)]	6360 (9900) [7760 (4830)]	6310 (10 400) [7760 (6600)]
$2^-$ C≡C	5860 (11 700) [~8000 (5600)]	5860 (5470) [~8000 (3580)] <sup>b</sup>	5760 (3200) [~8000 (3000)] <sup>b</sup>
$3^-$ N=N	9460 (22 200) [10 710 (18 900)]	9390 (22 500) [10 640 (18 500)]	9360 (17 000) [10 430 (14 260)]

<sup>a</sup>  $\nu = 0$  band maxima for delocalized species [in brackets:  $\nu = 1$  band maxima of delocalized species]. <sup>b</sup> The bump at  $\sim 8000 \text{ cm}^{-1}$  probably includes both localized and delocalized material.

tonian spectral analysis<sup>17,18</sup> using the four modes listed:  $h\nu/\text{cm}^{-1}$  (dimensionless distortion) 1470 (0.82), 1280 (0.68), 860 (0.81), 320 (0.94), with a line-broadening parameter  $\Gamma$  of  $914 \text{ cm}^{-1}$ . The spectra in DMF and in MeCN were fit by increasing  $\Gamma$  by 200 and  $400 \text{ cm}^{-1}$ , respectively, indicating that larger interactions with solvent are involved. The order of increased broadening is the same as that for increased  $\lambda_s$  for the localized species (see below).

**Dependence of  $\lambda$  on Solvent.** Although dielectric continuum theory has been widely used to estimate  $\lambda_s$  changes for class II intervalence compounds,<sup>4</sup> its assumptions that the only function of the bridge is to set the electron-transfer distance and that  $\lambda_s$  is proportional to the Marcus solvent parameter  $\gamma = n^{-2} - \epsilon_s^{-1}$  ( $n$  is the solvent refractive index and  $\epsilon_s$  the static dielectric constant) have been shown to be inadequate for class II hydrazine-centered intervalence radical cations.<sup>19,20</sup>  $\lambda_s(\text{MeCN})$  values at the same N, N distance vary widely depending upon whether the bridge is saturated or aromatic and also depend upon the structure of the charge-bearing unit. Furthermore,  $\lambda_s$  is higher for the high donor number solvents DMSO and DMF than it is in MeCN, although  $\gamma$  for DMSO and DMF is lower. The values of  $\lambda$  were shown to fit the double-parameter equation

$$\lambda = A + B\gamma + C(\text{DN}) \quad (1)$$

where DN is the Gutmann donor number<sup>21</sup> and the intercept  $A$  was interpreted as  $\lambda_v$ . The sign of the charge is also important in determining  $\lambda_s$ . It is clear from previous work<sup>13</sup> as well as this that for nitro-centered intervalence radical anions,  $\lambda_s$  is significantly smaller for the extremely high donor number HMPA than it is for MeCN and that  $\lambda_s(\text{CH}_2\text{Cl}_2)$  for  $2^-$  lies between those for DMSO and MeCN. These trends obviously have nothing to do with the dielectric continuum theory parameters  $n$  or  $\epsilon_s$  and appear to principally reflect the electron-accepting ability of the solvents. Therefore, IV band maxima  $h\nu_{IV} = \lambda$  values for the class II dinitro radical anions (summarized in Table 3) as a function of solvent were fit using the two-parameter eq 2,

$$\lambda = A + B\gamma + C(\text{AN}) \quad (2)$$

where AN is the Gutmann acceptor number. With the use of the solvent parameters shown in Table 2, the correlations obtained for these compounds are:

$$\lambda = 2150 + 4830\gamma + 240\text{AN} \quad \text{for } 1^- (\text{CH}=\text{CH}), \quad r = 0.90 \quad (2a)$$

$$\lambda = 1990 + 5920\gamma + 320\text{AN} \quad \text{for } 2^- (\text{C}\equiv\text{C}), \quad r = 0.98 \quad (2b)$$

The solvent-sensitive  $C(\text{AN})/(B\gamma + C(\text{AN}))$  ratios for  $1^-$  and  $2^-$  in acetonitrile are 0.64 and 0.66, so these dinitro radical anions are much more sensitive to the solvent electron-accepting ability than dihydrazine radical cations are to solvent donor ability (for a dozen systems, the  $C(\text{DN})/(B\gamma + C(\text{DN}))$  ratios in acetonitrile varied from 0.19 to 0.27).<sup>19</sup> Figure 6 displays the correlations and observed  $h\nu_{IV}$  data graphically. Fit to eq 1 is poorer for  $1^-$  (CH=CH) than for  $2^-$  (C≡C). The presence of significant amounts of delocalized material in the spectra of  $1^-$  may compromise the accuracy on the determination of the localized band maximum, because the second vibrational feature of the delocalized spectrum overlaps badly with the localized band maximum. Both compounds are clearly delocalized in HMPA, implying that  $H_{ab}$  must be greater than half of the 7100 extrapolated  $h\nu_{IV}$  value for  $1^-$  and about  $8000 \text{ cm}^{-1}$  for  $2^-$ .

We estimated  $\lambda_v$  for these systems using the calculated value of  $\lambda'_v$ ,<sup>23</sup> the enthalpy contribution to the vertical reorganization energy obtained from (U)B3LYP/6-31G\* calculations on 4-nitrostilbene, ( $3022 \text{ cm}^{-1}$ ) and 4-nitrotolane ( $3067 \text{ cm}^{-1}$ ). We initially planned to use nitrobenzene ( $\lambda'_v = 4850 \text{ cm}^{-1}$ ) as a model for both of these compounds, but the  $\lambda'_v$  calculated decreases as the size of the  $\pi$  system increases, and we believe that these estimates are more realistic. We have shown that calculations of  $\lambda'_v$  for monohydrazine<sup>0/+</sup> intermolecular electron-transfer reactions give  $\lambda'_v$  values that are only slightly larger than those calculated for intramolecular electron transfer within localized intervalence compounds having the same hydrazines as their charge-bearing units.<sup>24</sup> The size of the difference

(17) Zink, J. I.; Shin, K.-S. K. *Adv. Photochem.* **1991**, *16*, 119.

(18) Heller, E. J. *Acc. Chem. Res.* **1981**, *14*, 368–375.

(19) Nelsen, S. F.; Trieber, D. A., II; Ismagilov, R. F.; Teki, Y. *J. Am. Chem. Soc.* **2001**, *123*, 5684–5694.

(20) Nelsen, S. F.; Konradsson, A. E.; Teki, Y. *J. Am. Chem. Soc.* **2006**, *128*, 2902–2910.

(21) (a) Gutmann, V. *Coord. Chem. Rev.* **1976**, *28*, 225–255. (b) Gutmann, V. *The Donor–Acceptor Approach to Molecular Interactions*; Plenum: New York, 1980.

(22) Reichardt, C. *Solvents and Solvent Effects in Organic Chemistry*, 2nd ed.; VCH: Weinheim, Germany, 1988.

(23) Nelsen, S. F.; Blackstock, S. C.; Kim, Y. *J. Am. Chem. Soc.* **1987**, *109*, 677–682.

(24) Blomgren, F.; Nelsen, S. F. *J. Org. Chem.* **2001**, *66*, 6551–6559.

**Table 2.** Solvent Parameters Used in the Correlations<sup>a</sup>

solvent	$\gamma$	AN
MeCN	0.528	18.9
DMSO	0.437	19.3
DMF	0.463	16.0
HMPA	0.437	10.6
morph	0.337	17.5
PhCN	0.390	15.5
PhNO <sub>2</sub>	0.387	14.8
CH <sub>2</sub> Cl <sub>2</sub>	0.383	20.4
THF	0.375	8.0

<sup>a</sup> References 22 and 24.**Table 3.** Two-State Analysis of the Localized Spectra of **1**<sup>−</sup> and **2**<sup>−</sup>

compd (X)	solvent	$\lambda = h\nu_{IV}$	$\epsilon_{\max}$	$\Delta\nu_{1/2}$	$\mu_{12}$	$H_{ab}$	$2H_{ab}/\lambda$
<b>1</b> <sup>−</sup> CH=CH	MeCN	9680	2580	4630	3.08	545	0.11
	DMSO	8630	3350	5190	3.75	590	0.14
	morph	8190	3570	4930	3.87	580	0.14
	DMF	~7900	3260	5190	3.93	565	0.14
	PhNO <sub>2</sub>	~7810					
<b>2</b> <sup>−</sup> C≡C	MeCN	11300	3810	5050	3.61	750	0.14
	CH <sub>2</sub> Cl <sub>2</sub>	10800	3720	6230	3.95	780	0.14
	DMSO	10400	3570	5560	3.65	700	0.13
	DMF	9560	4050	6500	4.46	780	0.16
	PhCN	9230	7330	5880	5.61	935	0.20
	PhNO <sub>2</sub>	~9090					

increases as  $H_{ab}$  increases, because electronic coupling mixes the neutral and cation character of the hydrazine units. This calculation corresponds to an estimate of the maximum  $\lambda'_v$  values for localized versions of the intervalence compounds studied here. The effect of increasing basis set size on calculated  $\lambda'_v$  for neutral, radical cation couples has been shown to be rather small.<sup>25</sup> Comparing the unambiguously localized (because they show the broad Gaussian-shaped class II intervalence bands) **1**<sup>−</sup> and **2**<sup>−</sup> pair in MeCN,  $[h\nu_{IV}(C\equiv C) - h\nu_{IV}(CH=CH)] = 1520\text{ cm}^{-1}$ , indicating that  $\lambda_s$  is about that much larger for the tolane-bridged system, because the calculated  $\lambda_v$  values only differ by  $45\text{ cm}^{-1}$  for these compounds. The higher  $\lambda_s$  value for the C≡C-bridged compound is another effect on  $\lambda_s$  that is not predicted by dielectric continuum theory. Presumably, solvent can solvate the charge-bearing unit (including the C<sub>6</sub>H<sub>4</sub> ring attached to the reduced nitro group) of the C≡C-bridged compound more effectively than the CH=CH-bridged one, possibly because of less hindered approach. Rosokha et al. found a  $1730\text{ cm}^{-1}$  higher  $h\nu_{IV}$  for the C≡C-bridged dimethoxybenzene-centered radical cation than for the CH=CH-bridged one,<sup>26</sup> a trend in the same direction for an oppositely charged compound. The unambiguously delocalized (because they show the narrow spectra that exhibit vibrational fine structure) **1**<sup>−</sup> and **2**<sup>−</sup> pair in HMPA has  $h\nu_{IV}(CH=CH)$   $500\text{ cm}^{-1}$  larger than  $h\nu_{IV}(C\equiv C)$ . This is consistent with a larger  $H_{ab}$  for **A**(CH=CH) than **A**(C≡C) using the two-state model, which that is the conclusion of Barlow and co-workers for the related dianisylamine-centered radical cations. They assign the stilbene-bridged radical cation as delocalized, even in acetonitrile (a higher  $\lambda_s$

solvent for these radical cations) and the tolane-bridged one as localized even in methylene chloride (a lower  $\lambda_s$  solvent for cations).<sup>27,28</sup>

**Application of the Hush Two-state Model to the Class II Spectra.** The Hush two-state model with parabolic diabatic surfaces, which predicts the intramolecular electron-transfer rate constant surprisingly well for the localized 2,7-dinitronaphthalene radical anion,<sup>6</sup> has been applied to the localized spectra of **1**<sup>−</sup> and **2**<sup>−</sup>. The transition dipole moment  $\mu_{12}$  was calculated using Hush's Gaussian approximation<sup>29,30</sup> (eq 3)

$$\mu_{12} = n_{\text{cor}} 0.09584 (\epsilon_{\max} \Delta\nu_{1/2} / h\nu_{IV})^{1/2} \quad (3)$$

except that the Chacko refractive index correction  $n_{\text{cor}}$  has been included.<sup>31</sup> This correction,  $n_{\text{cor}} = 3n^{1/2}/(n^2 + 2)$ , has a value of 0.914 for MeCN, 0.890 for CH<sub>2</sub>Cl<sub>2</sub>, 0.872 for DMSO, 0.887 for DMF, 0.856 for PhCN, and 0.860 for DMPU. It is necessary to estimate the electron-transfer distance on the diabatic surfaces,  $d_{ab}$ , to obtain  $H_{ab}$  using Hush's eq 4. Although hybrid density functional

$$H_{ab} = (\mu_{12}/d_{ab})h\nu_{IV} \quad (4)$$

theory/Hartree–Fock UB3LYP calculations do an excellent job of calculating the optical spectra of class III intervalence compounds, including dinitroaromatic radical anions using Koopmans-based methods,<sup>11</sup> they overestimate the effects of electron delocalization and incorrectly delocalize many intervalence compounds that are localized.<sup>32</sup> Hartree–Fock calculations, which include no electron correlation, underestimate the effects of electron delocalization, and localize systems that are known to be delocalized. They incorrectly localize charge for gas-phase calculations on **1**<sup>−</sup> and give smaller dipole moments than seem likely to us. For this work, the  $d_{ab}$  required for (4) was calculated from  $d_{12}(\text{dm})$  using the semiempirical AM1 method for estimation of the dipole moment  $\mu_1$ , using  $d_{12}(\text{dm}) = 2\mu_1/4.8032$ , as previously discussed.<sup>33</sup> The small correction to convert the distance on the adiabatic surface which is calculated to that on the diabatic surface that is required for eq 4 was employed.<sup>33</sup> Both **1**<sup>−</sup> and **2**<sup>−</sup> give charge delocalization for AM1 calculations in the gas phase ( $\mu_1 = 0$ ), which is qualitatively correct, as demonstrated by their spectra showing the vibrational fine structure that is associated with charge delocalization in HMPA. The use of the conductor-like screening model (COSMO)<sup>34</sup> that is implemented in VAMP<sup>35</sup> caused charge localization accompanied by a rapid increase in  $\mu_1$  as the dielectric constant is increased; we used the values at  $\epsilon_s = 30$ , which produce  $d_{12} = 11.22\text{ Å}$  for **1**<sup>−</sup> and  $11.28\text{ Å}$  for **2**<sup>−</sup>,

- (25) Nelsen, S. F.; Weaver, M. N.; Pladziewicz, J. R.; Ausman, L.; Jentzsch, T. L.; O'Konneck, J. J. *J. Phys. Chem. A* **2006**, *110*, 11665–11676.  
 (26) Rosokha, S. V.; Sun, D. L.; Kochi, J. K. *J. Phys. Chem. A* **2002**, *106*, 2283–2292.

- (27) Barlow, S.; Risko, C.; Coropceanu, V.; Tucker, N. M.; Jones, S. C.; Levi, Z.; Khristalev, V. N.; Antipin, M. Y.; Kinnibrugh, T. L.; Timofeeva, T.; Marder, S. R.; Brédas, J.-L. *Chem. Commun.* **2005**, 764–766.  
 (28) Barlow, S.; Risko, C.; Chung, S.-J.; Tucker, N. M.; Coropceanu, V.; Jones, S. C.; Levi, Z.; Brédas, J.-L.; Marder, S. R. *J. Am. Chem. Soc.* **2005**, *127*, 16900–16911.  
 (29) Hush, N. S. *Prog. Inorg. Chem.* **1967**, *8*, 391–444.  
 (30) Hush, N. S. *Coord. Chem. Rev.* **1985**, *64*, 135–157.  
 (31) (a) Gould, I. R.; Noukakis, D.; Gomez-Jahn, L.; Young, R. H.; Goodman, J. L.; Farid, S. *Chem. Phys.* **1993**, *176*, 439–456. (b) Gould, I. R.; Young, R. H.; Albrecht, A. C.; Mueller, J. L.; Farid, S. *J. Am. Chem. Soc.* **1994**, *116*, 8188–8199.  
 (32) Blomgren, F.; Larsson, S.; Nelsen, S. F. *J. Comput. Chem.* **2001**, *22*, 655–664.  
 (33) Nelsen, S. F.; Newton, M. D. *J. Phys. Chem. A* **2000**, *104*, 10023–10031.  
 (34) Klamt, A.; Schüürmann, G. *J. Chem. Soc., Perkin Trans. 2* **1993**, 799.  
 (35) Clark, T.; Alex, A.; Beck, B.; Burkhardt, F.; Chandrasekhar, J.; Gedeck, P.; Horn, A. H. C.; Hutter, M.; Martin, B.; Rauhut, G.; Sauer, W.; Schindler, T.; Steinke, T. *VAMP 9.0*; Erlangen, 2003.

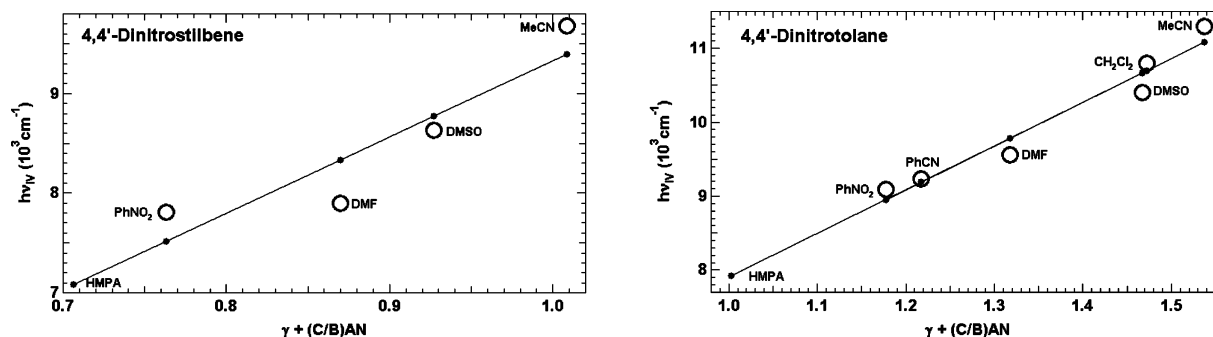


Figure 6. Plots of fits of band maxima for  $1^-$  and  $2^-$  to eq 2 showing the experimental data as circles.

Table 4. Koopmans-Based Band Positions and Intensities for the Radical Anions

compd	X	obsd type B	type B			type A		
		THF cm <sup>-1</sup>	calcd hv [f]	relative calcd hv	calcd – oβoδ	calcd hv [f]	relative calcd hv	calcd – oβoδ
$1^-$	CH=CH	6530	7110 [0.37]	≡0	+580	18920 [0.32]	≡0	+3760
$2^-$	C≡C	5860	6050 [0.37]	−1060	+190	21170 [0.34]	+2250	+6010
$3^-$	N=N	9460	10670 [0.32]	+3560	+1210	18800 [0.29]	−120	+430

which are 90% and 91% of the N, N distances, respectively.<sup>36</sup> The band widths at half-height for use in eq 3 were estimated for cases in which there is overlap with other bands. We summarize the two-state analysis of  $1^-$  and  $2^-$  in Table 3.

We included nitrobenzene as a quite easily reduced solvent when we discovered the rather high  $\lambda_s$  in methylene chloride for  $2^-$ , because we wanted to see if the low reduction potential for nitrobenzene would lead to anomalously high  $\lambda_s$  values for it. It does not, and  $h\nu_{IV}$  in nitrobenzene is near the lower limit of the localized spectra observed for both  $1^-$  and  $2^-$ . The  $H_{ab}$  values obtained using eqs 3 and 4 are all somewhat larger than the  $305 \pm 15$  cm<sup>-1</sup> obtained from a similar analysis of the non-Kekule-bridged 2,7-dinitronaphthalene radical anion, which has  $h\nu_{IV} = \lambda$  values of 9360 in MeCN, 8100 in DMF, and 8040 in PrCN.<sup>6</sup> The last column of Table 3 shows the values of  $2H_{ab}/\lambda$ , which is 1.0 at the point at which the barrier to electron transfer disappears and delocalization occurs. As can be seen in Figure 1, the sharper, lower energy spectral features associated with the delocalized species are clearly present in nitrobenzene, especially for  $1^-$ , implying that the energy difference between localized and delocalized material is so small that both are detectable in these solutions. Since according to the two-state model, delocalization occurs when  $H_{ab}$  exceeds  $\lambda/2$ , this implies that  $H_{ab}$  is actually about 3900 for  $1^-$  and somewhat less than 4500 for  $2^-$ . There is obviously a discrepancy between the  $H_{ab}$  values determined from the optical spectra and the point at which delocalization occurs, because the ratios are over a factor of 5 too small to be consistent with the appearance of the spectrum of delocalized material. Overestimation of the electron-transfer distance and radical anion decomposition would lead to  $H_{ab}$  values estimated from the class II spectra that are too small, but we doubt that our errors in these quantities would be that large. These results suggest to us that  $1^-$  and  $2^-$ , which are

obviously quite close to the class II/III borderline because solvent changes cause them to delocalize, are not being handled properly using the simple model. As the borderline is approached, the classical analysis Hush used requires that the band becomes increasingly cut off on the low-energy side because the band transition energy will not be less than  $\lambda/2$ .<sup>37–40</sup> The present data provide experimental confirmation that  $H_{ab}$  is significantly underestimated near the class II/III borderline. Kubiak and co-workers have also reported much smaller optical electronic couplings than are consistent with the very large rate constant measurements using IR line broadening for their oxo-bridge triruthenium cluster intervalence compounds.<sup>41</sup>

**Assignment of the Low-Energy Transitions.** With the use of the two-state model for the delocalized spectra in HMPA,  $H_{ab}$  in this solvent is  $h\nu_{IV}/2$ , or 3180 cm<sup>-1</sup> for  $1^-$  and 2930 cm<sup>-1</sup> for  $2^-$ , which is the opposite trend as that suggested from the solvent dependence of the spectra of these compounds in solvents in which localized material is observed, for which  $h\nu_{IV} = \lambda$  is significantly greater for  $2^-$  than for  $1^-$ . As pointed out previously for other dinitroaromatic radical anions<sup>11</sup> and discussed for the cases considered here immediately below, the lowest energy transition observed in the type III spectra of these compounds is not from the ground state to excited state of a single two-state model, so the class III transition energy should not be interpreted as twice an electronic coupling, despite the fact that this interpretation has been common in the literature. We shall employ Hoijtink's classification of optical bands of radical ions,<sup>42</sup> which designates filled orbital to singly occupied orbital (somo) transitions as type A, and somo to virtual orbital transitions as type B. More properly, type A transitions are  $\beta$ -(homo- $n$ ) to  $\beta$ (homo) and type B transitions are  $\alpha$ (homo) to

(36) The COSMO model uses only the solvent dielectric constant,  $\epsilon_s$ , to describe solvent effects. It makes the solvent effect directly proportional to the Kirkwood parameter,  $(\epsilon_s - 1)/(2\epsilon_s + 1)$ , as discussed previously for calculations on 2,7-dinitronaphthalene radical anion (ref 6).  $\epsilon_s$  dependence is obviously not sufficient to describe the solvent effects observed, because  $\epsilon_s$  is 29 for HMPA, but it clearly causes a lower  $\lambda_s$  than DMSO ( $\epsilon_s$  45), DMF ( $\epsilon_s$  37), and methylene chloride ( $\epsilon_s$  8.9) for the compounds under discussion.

(37) Lambert, C.; Nöll, G. *J. Am. Chem. Soc.* **1999**, *121*, 8434–8442.

(38) Nelsen, S. F. *Chem. Eur. J.* **2000**, *6*, 581–588.

(39) Demadis, K. D.; Hartshorn, C. M.; Meyer, T. J. *Chem. Rev.* **2001**, *101*, 2655–2685.

(40) Brunschwig, B. S.; Creutz, C.; Sutin, N. *Chem. Soc. Rev.* **2002**, *31*, 168–184.

(41) (a) Ito, T.; Hamaguchi, T.; Nagino, H.; Yamaguchi, T.; Kido, H.; Zavarine, I. S.; Richmond, T.; Washington, J.; Kubiak, C. P. *J. Am. Chem. Soc.* **1999**, *121*, 4625–4632. (b) Loneragan, C. H.; Salsman, J. C.; Lear, B. J.; Kubiak, C. P. *Chem. Phys.* **2006**, *324*, 57–62.

(42) Bally, T. In *Radical Ionic Systems*; Lund, A., Shiotani, M., Eds.; Kluwer: Dordrecht, The Netherlands, 1991; pp 3–54.

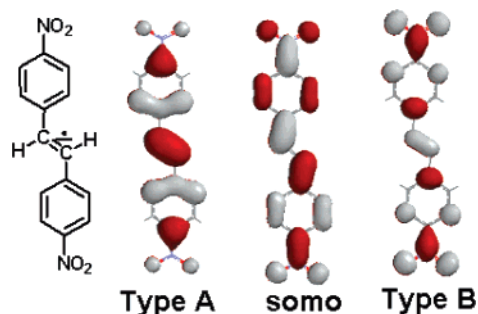


**Figure 7.** Orbitals involved in the lowest energy allowed type A and B transitions for  $1^-$ .

$\alpha(\text{homo}+n)$ , because an unpaired electron splits the degeneracy of all the orbitals and the “unpaired” electron is in an  $\alpha$  orbital. Calculated orbital energies can only meaningfully be compared for orbitals of the same occupancy. We have found that B3LYP calculations at the geometry of the radical ion with the somo filled (for the present compounds, dianion at anion geometry) produces filled orbital energy gaps that correlate with type A transitions rather well, and a calculation with the somo emptied (neutral at anion geometry) correlate with the type B transitions. Such Koopmans-based calculations have been carried out to consider the optical spectra of delocalized dinitroaromatic radical anions,<sup>11</sup> *p*-phenylene-bridged radical cations and anions,<sup>43</sup> and hydrocarbon radical cations.<sup>44</sup> These calculations can only consider delocalized, type III systems. The intervalence band for a type II system involves simultaneous promotion of an electron to and from the bridge (that is, overall transfer of an electron from one charge-bearing unit to the other), so its position cannot be estimated by a method that considers single-electron promotions.

The calculated band positions and oscillator strengths (*f*) are summarized in Table 4. The orbitals involved in the lowest energy allowed type A and type B transitions for the (CH=CH)-bridged  $1^-$  are shown in Figure 7 (the others are very similar; see the Supporting Information), and the calculated transition energies are compared visually with the observed spectra for  $1^-$  to  $3^-$  in Figures 8–10. Although TD–DFT calculations get significant configuration interaction for these low-energy transitions, both the transition energies and the relative band intensities are calculated better using the simple Koopmans-based model for these compounds. The first bands are type B, as for their analogues with smaller bridges.<sup>11</sup> The  $B_1$  bands of  $1^-$  to  $3^-$  are predicted an average of  $660\text{ cm}^{-1}$  too high (range  $1020\text{ cm}^{-1}$ ), close to what is obtained for the other delocalized dinitroaromatic radical anions studied.<sup>11</sup> Error increases as the transition energy increases, but the calculated order is the same as the observed one,  $X\equiv C < CH=CH < N=N$ . In contrast, TD–DFT calculations predict the first absorption band an average of  $3830\text{ cm}^{-1}$  too high (see the Supporting Information). The region of the second absorption bands is more complex than calculated by either method, which might be caused by the presence of decomposition products.<sup>42</sup> Type C bands usually become more important as transition energy increases, but TD–DFT calculations, which include such

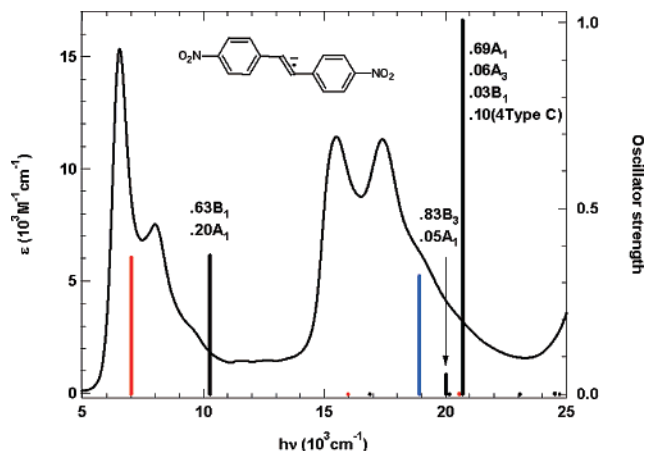


**Figure 8.** Comparison of Koopmans-based calculations on  $1^-$  (type A transitions are shown in blue and type B in red) and TD–DFT calculations (shown in black, with assignments) with its spectrum in THF.

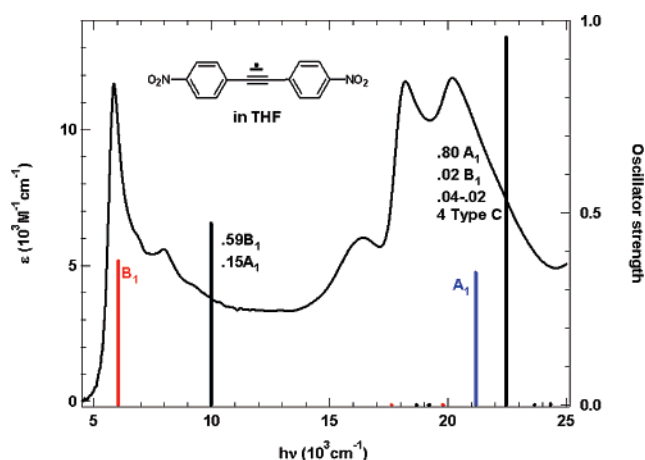


**Figure 9.** Same as Figure 8, except for  $2^-$ .

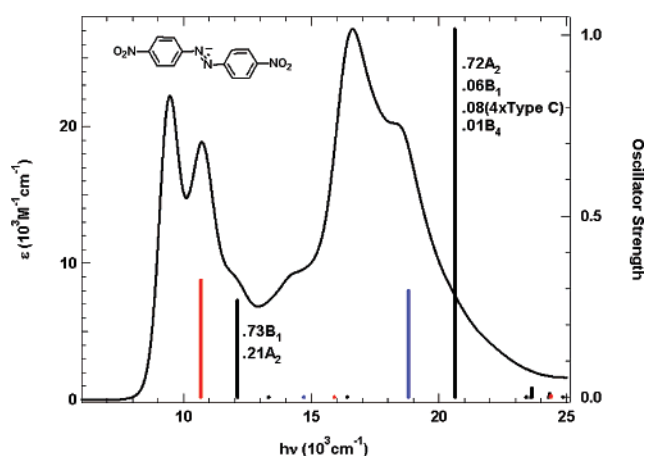


**Figure 10.** Same as Figure 8, except for  $3^-$ .

transitions, do not predict other bands with significant intensity for in the region below  $25\,000\text{ cm}^{-1}$ .

Since the Hush method for determining  $H_{ab}$  values from class II spectra in high  $\lambda_s$  solvents gives values that are significantly too small for these compounds, we instead tried to estimate values from calculations of their class III transitions in low  $\lambda_s$  solvents, using a neighboring orbital (NO) analysis. The details of this analysis for  $1^-$  to  $3^-$  only appear in the Supporting Information, because the analysis is rather complex and our

(43) Nelsen, S. F.; Weaver, M. N.; Telo, J. P.; Lucht, B. L.; Barlow, S. J. *Org. Chem.* **2005**, *70*, 9326–9333.

(44) Nelsen, S. F.; Weaver, M. N.; Bally, T.; Yamazaki, D.; Komatsu, K.; Rathore, R. J. *Phys. Chem. A* **2007**, *111*, 1667–1676.



conclusion is that the couplings obtained using it are not useful for predicting when delocalization will occur.

## Conclusions

Both the dinitrostilbene and dinitrotolane radical anions (**1**<sup>−</sup> and **2**<sup>−</sup>) show the spectra of delocalized intervalence compounds in HMPA and THF, but principally spectra of localized compounds in DMF, DMSO, and MeCN, with the transition energy at the band maximum (which is  $\lambda = \lambda_s + \lambda_v$ ) increasing in that order. Noncontinuum effects increase  $\lambda_s$  in better electron-accepting solvents for these intervalence radical anions, which is the opposite direction as the trends for intervalence radical cations, where  $\lambda_s$  is increased in electron-donating solvents. The electronic couplings ( $H_{ab}$ ) obtained by analysis of the intervalence bands for the localized spectra using Hush theory are far smaller than required for observation of charge localization in low  $\lambda_s$  solvents. The electronic couplings for **1**<sup>−</sup> and **2**<sup>−</sup> obtained from solvent effects on the spectra, assuming that the intervalence band maximum is the reorganization energy, which must be close to twice the electronic coupling when the energy difference between them is so small that significant amounts of both localized and delocalized material are observed, are  $\sim 3900\text{ cm}^{-1}$  for **1**<sup>−</sup> and somewhat less than  $4500\text{ cm}^{-1}$  for **2**<sup>−</sup>.

(45) Ruggli, P.; Lang, F. *Helv. Chim. Acta* **1938**, *21*, 38–50.

(46) Pausacker, K. H.; Scroggie, J. G. *J. Chem. Soc.* **1954**, 4003–4006.

(47) *Spartan '02*; Wavefunction, Inc.: Irvine, CA.

(48) Frisch, M. J.; et. al. *Gaussian 98*, revision A.9; Gaussian, Inc.: Pittsburgh PA, 1998.

Molecular orbital calculations show that the intervalence band for delocalized dinitroaromatic intervalence radical anions is not caused by a transition between the upper and lower states of a single two-state model, so the band maximum for delocalized intervalence compound should not be assumed to be twice the electronic coupling.

## Experimental Section

Compounds **1**,<sup>45</sup> **2**,<sup>45</sup> and **3**<sup>46</sup> were prepared according to known procedures. Their radical anions were prepared in vacuum-sealed glass cells equipped with an ESR tube and a quartz optical cell. The concentration of the samples (0.1–0.8 mM) was determined spectrophotometrically before reduction. Reduction was achieved by contact with 0.2% Na–Hg amalgam in the presence of an excess of [2.2.2]-cryptand (**6**).

The Koopmans-based spectral calculations used structures optimized using Spartan,<sup>47</sup> and the intensities were calculated using Gaussian 98.<sup>48</sup>

**Acknowledgment.** We are thankful for the financial support of this work from the National Science Foundation under Grant CHE-0240197 (SFN) and from Fundação Para a Ciência e Tecnologia through its Centro de Química Estrutural (J.P.T.).

**Supporting Information Available:** TD–DFT and neighboring orbital analysis for **1**<sup>−</sup> to **3**<sup>−</sup>; complete ref 48. This material is available free of charge via the Internet at <http://pubs.acs.org>.

JA067088M